Mineralogy, Trace Elements, and Rare Earth Element Composition of Sediments in an Amazonian Whitewater River: The Acre River

Alejandro Duarte[1,*], Enrique Roy Dionisio Calderon[2], Roberto R. de Avillez[2], Bruno Siciliano[2] and Adriana Gioda[2]

[1]*Universidade Federal do Acre, Centro de Ciências Biológicas e da Natureza, BR 364, Distrito Industrial, CEP 69920-900, Rio Branco, AC, Brazil*

[2]*Pontifícia Universidade Católica do Rio de Janeiro, Rua Marquês de São Vicente 225, Gávea, CEP 22451-900, Rio de Janeiro, RJ, Brazil*

Abstract: This study characterizes the mineralogical and geochemical composition of suspended (SS) and riverbed sediments (BS) from the Acre River, a whitewater tributary in Southwestern Amazonia. Four SS and four BS samples collected during the dry season were homogenized into composite samples and analyzed by different analytical techniques (ICP-MS, ICP OES, XRD, and FTIR). The results showed that quartz (up to 75 %) and kaolinite (up to 38 %) were the dominant minerals, together with feldspars and TiO_2. Rare earth elements (REEs) were present at low to moderate concentrations (0.11-52 μg g^{-1}), with Ce and La being the most abundant. Trace elements such as V, Ni, Ga, Rb, and Cs showed enrichment relative to upper continental crust. Although the single-season sampling limits temporal interpretation, comparison with published datasets from the Purus and Solimões basins suggests that both natural weathering and local land-use pressures influence sediment composition. These results provide new geochemical data for a poorly studied Amazonian tributary and contribute to the broader understanding of sediment provenance and hydrogeochemical processes in whitewater rivers.

Keywords: Acre river, Amazon basin, Hydrogeochemistry, Rare earth elements, Sedimentology, Whitewater.

1. INTRODUCTION

The Amazon Basin is an exceptionally complex biome in which the biosphere, hydrosphere, atmosphere, lithosphere, and cryosphere interact continuously, shaping processes that operate from local to global scales. The Amazon rainforest plays a central role in sustaining the planet's climatic equilibrium through its regulation of energy, water, and biogeochemical cycles. Studies have examined the basin to understand the functioning of natural cycles and the mechanisms that govern material fluxes and environmental transformations. In this context, river discharge and sediment transport are key components, reflecting biogeochemical processes driven by erosion and weathering across mountainous regions, soils, and floodplains [1].

The geological and geomorphological contrasts between the Andes and the Guiana Shields define two major hydrographic domains: whitewater and blackwater systems. Whitewater rivers originate predominantly in Andean and Sub-Andean terrains and are influenced by large tributaries such as the Solimões and Madeira rivers. Blackwater rivers, in contrast, characterize northern Amazonia, draining highly weathered soils and following the course of the Negro River before its confluence with the Solimões [2].

*Address correspondence to this author at the Universidade Federal do Acre, Centro de Ciências Biológicas e da Natureza, BR 364, Distrito Industrial, CEP 69920-900, Rio Branco, AC, Brazil;
E-mail: fd.alejandro@gmail.com

These differences in origin and landscape are reflected in distinct organic matter signatures: the Negro River contains high concentrations of colloidal organic carbon, whereas the Solimões River carries predominantly dissolved and particulate organic carbon. The contrasting contributions are linked to the soil types eroded by each system. Blackwater rivers typically mobilize podzol, ferralsol, and acrisol soils, while whitewater rivers drain a broader diversity of soil classes, including acrisols, ferralsols, nitisols, cambisols, vertisols, luvisols, and plinthosols, characteristic of western and southern Amazonia [3-5].

Numerous studies have examined the mineralogical and geochemical characteristics of large Amazonian rivers, especially in central Amazonia, where sediment contributions from the Andes dominate [6–10]. However, most existing data are concentrated in mainstem rivers and central floodplain regions, while several southwestern tributaries remain poorly characterized. Understanding sediment composition in these tributaries is essential for identifying geochemical signatures, assessing weathering processes, and evaluating natural versus anthropogenic influences on riverine materials [11-14]. This is particularly relevant given ongoing land-use changes, population expansion, and increasing agricultural pressure in southwestern Amazonia, which may alter sediment fluxes and chemical loads.

Among the understudied systems, the Acre River, a whitewater tributary of the Purus River, stands out due

Received on 18-10-2025 Accepted on 24-11-2025 Published on 27-11-2025

E-ISSN: 2311-8741/25

to its strategic location between Andean headwaters and central Amazonian floodplains. Despite its hydrological and socio-environmental importance, there is a lack of integrated mineralogical and geochemical data, especially concerning the distribution of rare earth elements (REEs) and trace elements. Therefore, the objective of this study is to characterize the mineralogical composition and the concentrations of major, trace, and REEs in suspended and riverbed sediments of the Acre River. The novelty of this work lies in providing one of the first datasets of this kind for a southwestern Amazonian tributary, contributing to the understanding of sediment provenance and geochemical processes in an understudied region of the basin.

2. MATERIALS AND METHODS

2.1. Study Area

This study was conducted in August 2018, during a single dry-season campaign, when four riverbed sediment (BS) and four suspended sediment (SS) samples were collected from the Acre River at coordinates 9° 58' 45" S and 67° 48' 30" W (Figure **1**). Sampling restricted to one hydrological period does not allow evaluation of seasonal variability, which may influence sediment composition due to changes in rainfall, river discharge, flood dynamics, and sediment resuspension. Therefore, the results presented here represent dry-season conditions, and temporal variability remains a limitation of the dataset.

2.2. Chemical Analysis

Inductively Coupled Plasma Mass Spectrometry (ICP-MS), Inductively Coupled Plasma Optical Emission Spectrometry (ICP OES), X-ray Powder Diffraction (XRD), and Fourier Transform Infrared Spectroscopy (FTIR) were employed to determine the chemical and mineralogical composition of SS and BS samples. XRD and FTIR were used to identify mineral phases and assess structural characteristics associated with weathering and sediment provenance. Element concentrations in sediment samples are reported in μg g^{-1} (dry weight basis), while concentrations in digested solutions are expressed in μg L^{-1}.

2.2.1. Inductively Coupled Plasma Mass Spectrometry (ICP-MS)

Four riverbed sediment samples were collected using a stainless-steel spatula, and four water samples were collected in 1-L plastic bottles at approximately 20 cm below the river surface. After several days of settling, the supernatant water was carefully decanted to isolate the suspended sediments. All sediment samples (SS) were dried in a controlled laboratory environment. The SS samples were milled, sieved, and homogenized prior to their acid extraction. Approximately 0.15 g of sediment was weighed in triplicate. About 0.01 g of certified reference material (CRM, NIST SRM 2704 Buffalo River Sediment, NIST SRM 88b Dolomitic limestone, NIST SRM 1648a Urban

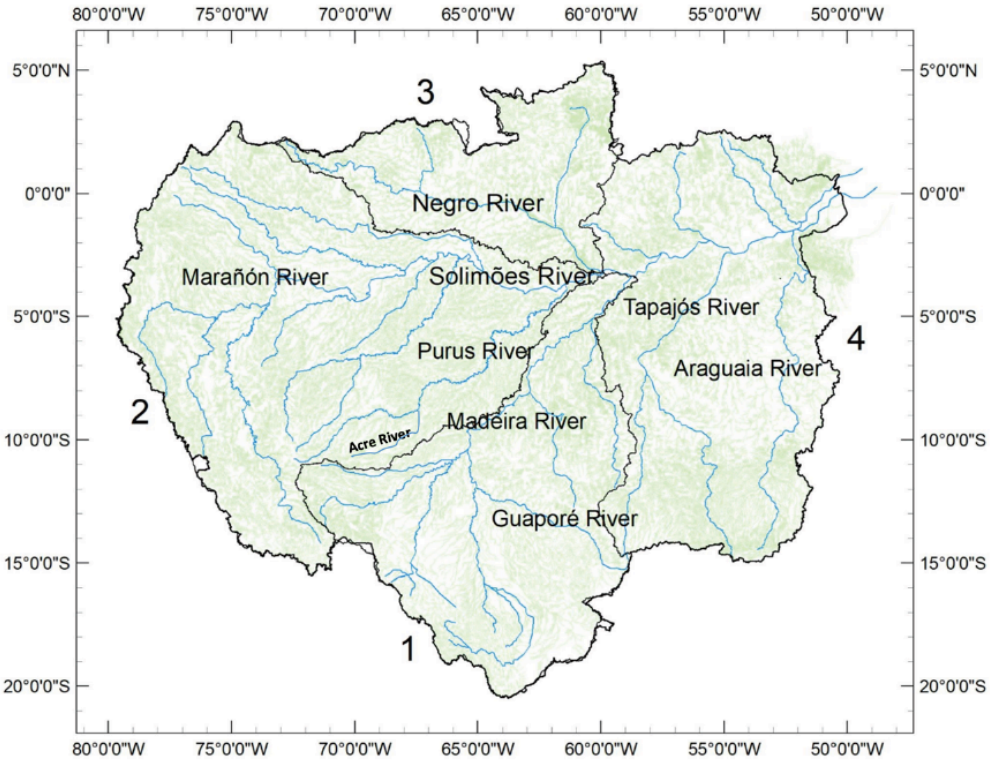

Figure 1: Four catchments of the Amazon basin: **1** and **2**) whitewater rivers: Madeira River and Solimões River, respectively; **3**) blackwater rivers: Negro River; **4**) clearwater rivers: Tapajós River. Each catchment was identified by its principal rivers.

Particulate Matter) was weighed and analyzed in parallel. The samples were transferred to Savillex Teflon bottles, and 3.0 mL of bidistilled hydrochloric acid (HCl), 1.0 mL of bidistilled nitric acid (HNO_3) (65 %) and 0.2 mL of hydrofluoric acid (HF) were added. The samples were heated at 150 ºC for 4 h. Afterwards, the Teflon bottles were opened, and 1.0 mL of HNO_3 was added to promote the evaporation of HF. Finally, the extracts were diluted and analyzed.

The chemical composition of trace elements in the samples was determined using inductively coupled plasma mass spectrometry (ICP-MS, NexIon 300X, PerkinElmer, Canada). Rhodium (^{103}Rh) was used as an internal standard (IS) to reduce non-spectral interferences and matrix effects. The quantification of the elements was performed using an external analytical curve of twelve points. The concentrations used in the analytical curves ranged from 0.5 μg L^{-1} (minimum value for Au) to 1980 μg L^{-1} (for major elements such as Fe, Ca, K, Mg, Na). The instrumental limit of detection varied from 0.145 μg L^{-1} (for Re) to 267 μg L^{-1} (for Ca), while the instrumental limit of quantification ranges from 0.467 μg L^{-1} (for Re) to 882 μg L^{-1} (for Ca). ICP-MS is widely recognized for its high sensitivity, especially in the determination of REEs and other trace metals in sediment samples, supporting its use in this study [15–17].

2.2.2. Inductively Coupled Plasma Optical Emission Spectrometry (ICP OES)

The chemical composition of major elements was determined using inductively coupled plasma optical emission spectrometry (ICP OES, Optima 4300 DV, Perkin Elmer, USA). The SS samples were dried, milled, sieved, and homogenized prior to their acid extraction. Approximately 50 mg of the sample was weighed and mixed with 500 mg of lithium metaborate, used as flux. The mixture was then melted into a platinum crucible. A gas burner was used to melt the mixture until a homogeneous and transparent liquid was obtained. The glass pellet was then dissolved with 50 mL of HNO_3 (10 %). About 0.01 g of certified reference material (CRM, NIST SRM 2704 Buffalo River Sediment, NIST SRM 88b Dolomitic limestone, NIST SRM 1648a Urban Particulate Matter) was weighed and prepared in the same way to be later analyzed in parallel.

2.2.3. X-ray Powder Diffraction (XRD)

The mineralogical composition of the SS and BS samples was analyzed by X-ray powder diffraction using a D8-Discover (Bruker), with Bragg-Brentano geometry, a Cu tube, a Kβ Ni filter, and a LynxEye detector (Bruker). The 2θ scan was set from 5° to 80°, with a 0.02° 2θ step. The acquisition time was adjusted to get approximately 10000 counts for the main peak. The minerals were identified with EVA (Bruker) program and the ICDD (International Centre for Diffraction Data) 2003 database. Quantitative analysis was performed with the Profex [18], a graphical interface for the Rietveld fitting using the BGMN program with fundamental parameters.

2.2.4. Fourier Transform Infrared Spectroscopy (FTIR)

The analyses of SS samples were performed using a spectrometer, model 100 FTIR (Perkin-Elmer, USA), with data collected in the region of 4000-450 cm^{-1}. The SS samples were analyzed using the potassium bromide (KBr) pellet technique at room temperature. Quantitative and qualitative data from FTIR spectroscopy analyses were compared to those by XRD, ICP-MS and ICP OES to assess the elemental composition of the sediments and their association with specific mineral phases.

2.3. STATISTICAL ANALYSIS

ICP-MS and ICP OES datasets were processed using the R statistical environment (version 1.1.447; RStudio). Correlation matrices and hierarchical clustering were generated using the *corPlot* package to identify relationships among chemical variables.

Anthropogenic influence on SS composition was assessed using the enrichment factor (EF), calculated according to Equation (1). Element concentrations in sediments (X_i) and upper continental crust (UCC) reference values were normalized to scandium (Sc), a conservative lithogenic element widely employed for EF [19].

$$EF_i = \frac{\left({}^{X_i}/_{Sc}\right)_{SS}}{\left({}^{X_i}/_{Sc}\right)_{ref}} \quad (1)$$

Scandium was selected as the normalizing element because it is a refractory, lithogenic trace element that is largely insoluble and exhibits minimal mobility during sedimentary processes. Its concentration is only weakly influenced by chemical or physical weathering, mineral sorting during transport, or dilution by dominant phases such as quartz, organic matter, or carbonates [19, 20]. The enrichment factor (EF) provides an estimate of how much the concentration of a given element deviates from its expected natural abundance. In this study, EF values indicate whether an element is enriched or depleted in Acre River suspended sediments relative to upper continental crust, reflecting the combined effects of weathering, erosion, secondary mineral formation, and other geochemical processes

acting within the basin.

3. RESULTS

3.1. Chemical Composition of the Suspended Sediment

The concentrations of the most abundant major and trace elements in the SS samples, including rare earth elements (REEs), are presented in Table **1** (ICP-MS results) and Table **2** (ICP OES results).

Table 1: ICP-MS Results for Suspended Sediment (SS) Concentrations of Rare Earth Elements (REEs) and Enriched Trace Elements ([SS], μg g^{-1}), and Associated Analytical Uncertainties (δ)

Element	[SS] (μg g^{-1})	δ (μg g^{-1})
Li	93	7
Be	1.5	0.1
Na	2,466	147
Mg	6,111	333
Al	Saturated [a]	-
Si	572	663
K	Saturated	-
Ca	7,366	315
Sc	14	2
Ti	941	81
V	144	9
Cr	71	5
Mn	1034	57
Fe	50	2
Co	18	1
Ni	33	2
Cu	26	2
Zn	93	12
Ga	47	3
Ge	0.8	0.1
As	11	0.8
Se	< LOQ [b]	-
Br	6	0.9
Rb	161	11
Sr	121	9
Y	13	1
Zr	27	2
Nb	3	0.3
Mo	0.8	0.1
Ag	0.9	0.1
Cd	0.2	0.02
Sn	2.6	0.2
Sb	0.5	0.1
Cs	10.3	0.6
Ba	699	48
La	27	2
Ce	52	3
Pr	5.6	0.3
Nd	21	1
Sm	5.1	0.3
Eu	1.3	0.1
Gd	4.8	0.3
Tb	0.59	0.05
Dy	2.5	0.2
Ho	0.44	0.02
Er	1.1	0.1
Tm	0.14	0.01
Yb	0.84	0.06
Lu	0.11	0.01
Ta	0.051	0.005
Au	< LOQ	-
Tl	0.42	0.03
Pb	12	1
Bi	0.143	0.009
Th	4.8	0.3
U	0.76	0.05

[a] "Saturated" indicates concentrations exceeding the instrument's detection range.

[b] "< LOQ" indicates concentrations below the limit of quantification.

Table 2: ICP OES Results for Suspended Sediment (SS) Concentrations of Major Elements ([SS], μg g^{-1}), and Associated Analytical Uncertainties (δ)

Element	[SS] (μg g^{-1})	δ (μg g^{-1})
Na	< LOQ [a]	47
Mg	6,601	122
Al	86,622	1,635
Si	252,779	3,604
S	< LOQ	50
K	16,614	984
Ca	5,856	181
Ti	5,512	75
V	< LOQ	5
Cr	53	8
Mn	845	13
Fe	45,062	915
Zn	132	25
Ba	557	17

[a] "< LOQ" indicates concentrations below the limit of quantification.

In the SS samples, the ICP-MS data show the

following increasing order of concentrations: Ta < Lu < Tm < Bi < Cd < Tl < Ho < Sb < Tb < U < Ge < Yb < Mo < Ag < Er < Eu < Be < Dy < Sn < Nb < Th < Gd < Sm < Pr < Br < Cs < As < Pb < Y < Sc < Co < Nd < Cu < La < Zr < Ni < Ga < Ce < Cr < Zn < Li < Sr < V < Rb < Si < Ba < Ti < Mn < Na < Mg < Ca < Fe < Al ≈ K. For the ICP OES data, the order is: Cr < Zn < Ba < Mn < Ti < Ca < Mg < K < Fe < Al < Si (with minor differences in the relative position of Ti and Mn). It is important to note that several elements were quantified by both ICP-MS and ICP OES, and some discrepancies were observed between the two datasets. These differences primarily reflect the distinct digestion procedures and analytical sensitivities of each technique, which can favor the recovery of specific elements over others. For comparative purposes, the values associated with the highest and most consistent recoveries were selected, except in cases where the higher concentration exceeded the instrumental linear range, indicating potential signal saturation.

It is noteworthy that all REEs (La, Ce, Pr, Nd, Sm, Eu, Gd, Tb, Dy, Ho, Er, Yb, Lu, and Sc and Y) were detected in the Acre River SS. This extensive detection aligns with broader basin-scale studies; for example, previous work has shown that REEs are measurable in both dissolved and particulate phases of the Amazon River and its major tributaries [13]. Most detrital minerals naturally incorporate REEs, typically with a predominance of Ce and La [21]. This pattern is evident in Figure **2**, where these element concentrations in Acre River SS are compared with data of the Solimões and Amazon rivers. A clear downstream enrichment is observed: REE concentrations increase by approximately 3.5-fold from Acre to the Solimões and nearly 7-fold from Acre to the Amazon, particularly for elements from La to Nd. This progressive enrichment reflects the increasing contribution of fine-grained sediments carrying REE-bearing mineral phases, as well as hydrodynamic sorting processes that preferentially transport these minerals downstream. The dominance of Ce and La aligns with the characteristic REE signatures reported for tropical river suspended loads. These trends highlight the strong influence of sediment provenance and transport dynamics on REE distribution along the Acre-Purus-Solimões-Amazon continuum. It is also important to emphasize that REE data for Amazonian sediments remain scarce, especially for tributaries of the Solimões River, underscoring the relevance of the present dataset [13].

3.2. Enrichment Factor

The results better characterize compositional variations in surface suspended solids, especially in shallow rivers where particle size reflects a mix of riverbed and surface sediments. Figure **3** shows the enrichment factor for various elements present in the Acre River SS chemical compositions.

3.3. FTIR and XRD Mineralogical Characterization of BS and SS

The FTIR spectrum of the Acre River suspended sediments (Figure **4**) indicates the presence of quartz, aragonite, calcite, kaolinite, smectite, hematite, and feldspar. These mineral phases are consistent with the elemental composition obtained by ICP-MS and ICP OES and with the crystalline phases identified through XRD, as discussed below.

The FTIR spectrum follows the typical patterns

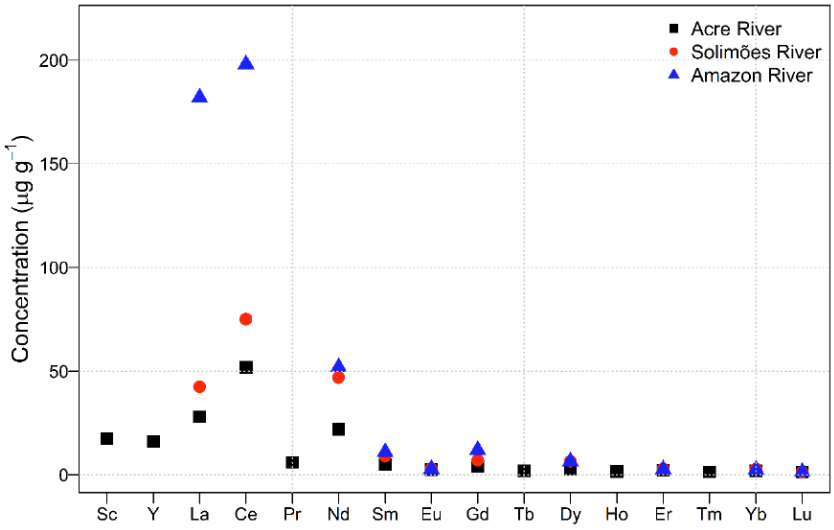

Figure 2: Chemical concentrations of rare earth elements (REEs) in suspended sediments (SS) from the Acre (black squares), Solimões (red circles), and Amazon (blue triangles) Rivers, expressed in µg g^{-1}.

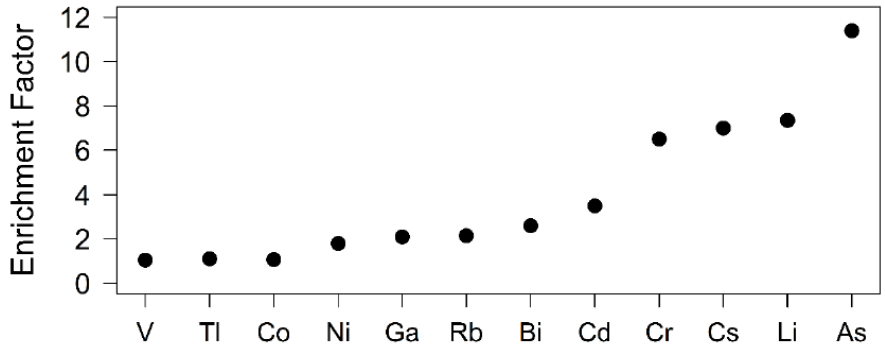

Figure 3: Enrichment factor (EF) values of the 12 enriched elements identified in suspended sediments (SS) from the Acre River, calculated using upper continental crust (UCC) reference concentrations.

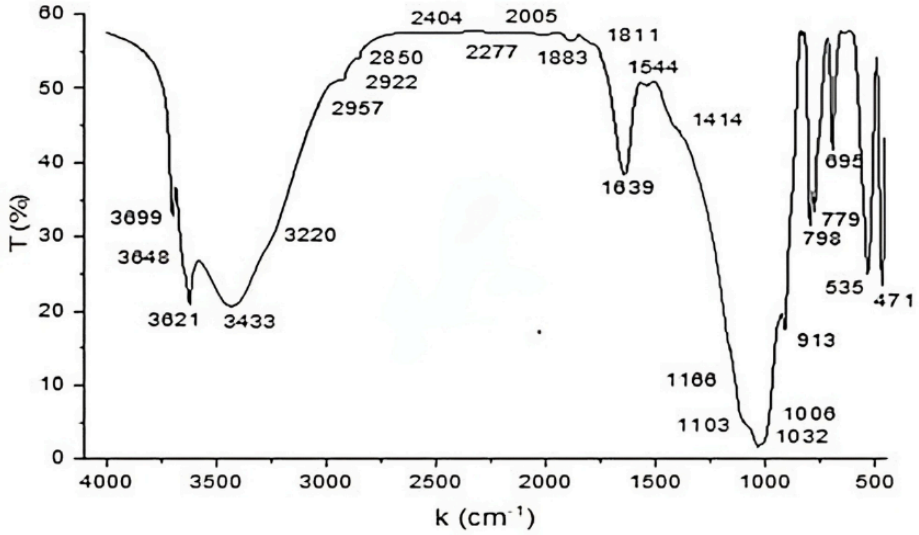

Figure 4: FTIR absorption spectrum of suspended sediments (SS) from the Acre River, indicating minerals such as quartz, feldspars, and kaolinite.

reported in the literature [22, 23]. Quartz is identified by characteristic absorption bands near 695, 779, 798, 1032, 1166, and 1883 cm^{-1}. Feldspars, orthoclase, microcline, and Na- and Ca-plagioclases, exhibit absorptions around 535, 1006, and 1032 cm^{-1}, reflecting their similar aluminosilicate structures. Kaolinite is detected by diagnostic bands at 913, 1032, 1103, 3621, 3648, and 3699 cm^{-1}, while broader bands at ~3400 and ~1640 cm^{-1} suggest a less ordered kaolinite structure. Organic matter is evidenced by C–H stretching bands at approximately 2850 and 2922 cm^{-1}. Additionally, absorption between 470 and 799 cm^{-1} supports the presence of kaolinite, consistent with observations by Moreira-Turcq *et al*. [24].

The XRD diffractograms (Figure **5**) further confirm the dominance of quartz and kaolinite. The calculated Rietveld refinement profiles and residuals indicate good fit quality. Bergmann's kaolinite structural model [25] was applied during refinement. Quartz exhibits highly intense peaks, particularly at $2\theta \approx 26.66°$, where counts reached 9181.39 for the riverbed sediment (BS) and 5436.08 for the suspended sediment (SS), reflecting its dominance in both fractions. A few unidentified peaks slightly above background were observed but not included in the refinement due to their very low intensity. Based on the Rietveld results, BS samples contain 58.8 % quartz and 37.9 % kaolinite (Figure **5a**), with refinement statistics of Rwp = 7.50 % and a goodness-of-fit of 1.1924, indicating a robust fit. In contrast, SS samples exhibit 74.6 % quartz and 16.0% kaolinite (Figure **5b**), with Rwp = 8.38% and a goodness-of-fit of 1.1954. These results confirm that SS is more enriched in quartz relative to BS, consistent with the preferential transport of fine quartz-rich particles in suspension. The crystalline phases identified in SS (Table **3**) include quartz (SiO_2), kaolinite ($Al_2Si_2O_9$), and Ti-bearing oxides such as rutile (TiO_2) and anatase (TiO_2). In BS, additional elements, H, O, Na, Mg, Al, Si, P, Ca, Ti, and Fe, were also detected, suggesting the presence of other mineral phases at concentrations below the XRD detection threshold.

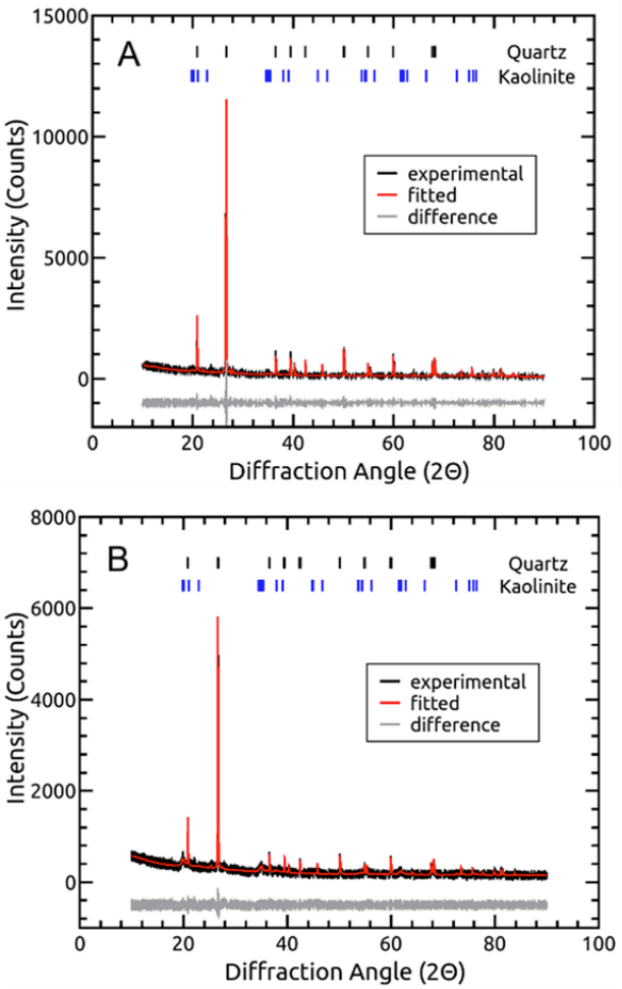

Figure 5: X-ray diffraction patterns of (a) suspended sediment (SS) and (b) riverbed sediment (BS) from the Acre River. Experimental data are shown in black, Rietveld-fitted profiles in red, and the difference between experimental and fitted patterns in gray. Vertical tick marks indicate the positions of quartz (black) and kaolinite (blue) diffraction peaks.

Table 3: Mineral Composition of Riverbed (BS) and Suspended Sediments (SS). Values are Expressed as Weight Percentages

Mineral	Chemical Formula	BS (%)	SS (%)
Quartz	SiO_2	74.59	58.8
Kaolinite	$Al_2Si_2O_5(OH)_4$	16.00	37.9
Diopside	$Fe_{0.26}Mg_{0.74}CaSi_2O_6$	2.73	–
Titanite	$CaTiSiO_5$	0.58	–
Newberyite	$MgHPO_4{\cdot}3H_2O$	2.25	–
Albite	$NaAlSi_3O_8$	3.45	–
Anatase	TiO_2	0.39	1.51
Rutile	TiO_2	–	1.83

The detected elements are likely associated with the main mineral phases identified (quartz, kaolinite, feldspars, and Ti-oxides). However, their distribution also suggests the possible presence of additional mineral phases such as albite ($NaAlSi_3O_8$), diopside ($Fe_{0.26}Mg_{0.74}CaSi_2O_6$), newberyite ($MgHPO_4{\cdot}3H_2O$), and titanite ($CaTiSiO_5$). These phases may remain undetected by XRD when present at mass fractions below approximately 1%, which is below the typical detection limit of the technique. Low-intensity peaks observed between 2θ = 3° and 20° were interpreted as contributions from clay minerals. This range is consistent with the presence of illite and other layered silicates, which have been reported as significant components of fine sediments in the Purus Basin, of which the Acre River is a tributary.

4. DISCUSSION

4.1. Acre River SS Elemental Concentration

The SS load of the Acre River displays the typical composition of whitewater systems, which are dominated by fine mineral particles transported from Andean-derived terrains. These sediments naturally incorporate a wide range of major and trace elements; however, the EF analysis enables discrimination between natural geochemical background and human-driven inputs. In this study, EF values indicate clear anthropogenic enrichment for several elements, specifically V, Tl, Co, Ni, Ga, Rb, Bi, Cd, Cr, Cs, Li, and As. Because EF normalizes concentrations to a conservative lithogenic element (Sc) and compares them to upper continental crust, elevated EF values cannot be attributed to natural weathering alone. Instead, they signal human influence. In the Acre River Basin, such enrichment is likely associated with land-use change, soil exposure, agricultural inputs (including fertilizers and agrochemicals), road construction, urban expansion, and the influx of atmospheric pollutants transported from other regions of Amazonia. The enrichment of potentially toxic elements such as Cd, Cr, Ni, Tl, and As is of particular concern, as these elements can become mobile and bioavailable in fine suspended particles. The dominance of fine-grained SS enhances downstream transport efficiency, increasing the potential for dispersion of anthropogenic contaminants across the basin. This reinforces the importance of continuous monitoring and geochemical surveillance in southwestern Amazonia, where detailed sediment-quality assessments remain scarce.

An additional point of interest is the absence of detectable Hg. Although the Acre River Basin itself is not a major center of Hg release, neighboring regions, especially the Madeira Basin, experience significant inputs from artisanal gold mining and biomass burning. Given this regional context, the lack of Hg detection in SS is somewhat unexpected, though it may reflect low background levels in this specific tributary, hydrological seasonality, or effective retention within soils rather than in the suspended load.

Altogether, the geochemical patterns observed in the Acre River sediments highlight not only their mineralogical affinity with Andean-derived materials but also the influence of contemporary anthropogenic pressures on the distribution of trace metals. These findings underscore the need for more comprehensive spatial and temporal assessments to improve understanding of human impacts on sediment quality in the southwestern Amazon Basin.

4.2. Natural and Anthropogenic Sources of REEs in the SS

All 16 naturally occurring REEs were detected in the SS of the Acre River Basin. This raises important questions regarding their sources, particularly given the global increase in REE production driven by agricultural, technological, and industrial demands. Although REEs are widely dispersed in the environment, their concentrations in river systems can be influenced by both natural and anthropogenic processes. As of 2025, Brazil holds one of the largest known REE reserves worldwide, approximately 21 million tonnes, ranking second only to China [26].

REEs are commonly classified into two groups, light REEs (LREEs, La–Eu) and heavy REEs (HREEs, Gd–Lu), or, in some frameworks, into three groups: LREEs (La–Sm), medium REEs (MREEs, Eu–Tb), and HREEs (Dy–Lu) [27]. Their environmental behavior often varies across these groups due to differences in ionic radii, complexation capacity, and affinity for mineral phases.

Phosphate fertilizers represent a relevant anthropogenic source of REEs. These products frequently contain elevated concentrations of LREEs, especially Ce and La, due to the natural enrichment of REEs in phosphate ores [28]. In Brazil, phosphate fertilizers may contain Ce concentrations as high as 1,499 μg g^{-1} [20], making them potential contributors to REE accumulation in agricultural soils and, consequently, to their transfer into rivers via runoff. REEs are also commonly associated with natural phosphates and carbonates [29-31], which may enter river systems through soil erosion and mineral weathering. In the Acre River Basin, agricultural expansion, particularly for soybean and corn cultivation, has increased the application of superphosphates and limestone, both of which can contain REEs. These agricultural inputs constitute potential anthropogenic sources in local ecosystems. Although plant uptake of REEs is generally regulated by physiological mechanisms, the extent of transfer from soil to vegetation depends on factors such as REE speciation, soil concentration, pH, and adsorption behavior [27, 32].

Alongside these anthropogenic contributions, natural processes such as erosion of REE-bearing soils and weathering of rocks provide a continuous background supply of REEs to the river system. The combined influence of natural geology and agricultural intensification helps explain the REE patterns observed in the Acre River suspended sediments, highlighting agriculture as a significant and emerging source of REEs in the region.

4.3. Mineralogical Composition of the Sediments

The integration of chemical and mineralogical data on sediments transported throughout the Amazon Basin provides a clearer understanding of the processes that shape the composition of whitewater rivers and ultimately the massive sediment load delivered by the Amazon River. Chemical weathering plays a central role in this system, transforming primary minerals into secondary oxides within soils, waters, and biomass, while chemical denudation transports dissolved and particulate materials downstream through groundwater and river flows [33].

Table **4** summarizes the concentrations (%) of major oxides in sediments from different sectors of the basin, which form the basis for the clustering patterns shown in Figure **6** [11]. These clusters highlight the similarity among whitewater river systems and exclude the chemically distinct blackwater system of the Negro River. The lowest oxide concentrations correspond to sediments found downstream of the confluence between the Negro and Solimões rivers, reflecting dilution effects and the distinctive geochemistry of blackwater contributions. In contrast, the Amazon mainstream suspended sediments are enriched in Si, Al, and Fe, followed by K, Mg, Ca, Na, Mn, and Ti, consistent with the dominance of quartz, aluminosilicate minerals, and Fe-bearing phases.

The mineralogical and geochemical patterns observed in the Acre River Basin align with those found across other whitewater tributaries, reflecting their shared geological origin and the influence of similar soil types across the Andean and Sub-Andean regions [34]. The enrichment of REEs in these sediments reflects a long-standing history of mineral transformation, weathering, and sediment transport across the basin [35].

Current environmental pressures, particularly deforestation and biomass burning, have become increasingly relevant in shaping sediment dynamics in Amazonia. These processes modify local and regional rainfall patterns, enhance soil erosion, and alter the flux and composition of suspended and riverbed sediments transported by rivers. As these disturbances intensify,

Table 4: Concentration of Oxides in Rivers along the Amazon Basin, Expressed as Percentages of Total Sediment. Adapted from Martinelli *et al*. [11]

SiO_2	Al_2O_3	Fe_2O_3	Na_2O	CaO	K_2O	MgO	TiO_2
65.15	16.38	5.77	4.20	3.30	2.43	1.79	0.98
64.57	16.39	5.60	4.78	3.44	2.53	1.75	0.94
64.95	16.91	5.97	3.87	3.16	2.32	1.81	0.99
65.84	15.94	5.96	3.78	3.22	2.50	1.73	1.02
68.66	15.09	5.05	3.76	2.75	2.27	1.50	0.93
67.13	15.89	5.81	3.42	2.72	2.41	1.58	1.04
66.48	16.22	5.76	3.47	2.93	2.46	1.65	1.02
63.79	17.35	6.11	4.27	3.29	2.36	1.79	1.03
67.30	16.09	5.73	3.15	2.61	2.49	1.60	1.02
67.80	15.57	5.41	3.52	2.98	2.18	1.61	0.94
66.88	15.73	5.37	4.03	3.10	2.40	1.49	0.99
65.00	17.11	6.11	3.61	2.80	2.63	1.65	1.08
73.79	13.36	5.20	2.18	1.37	2.12	1.02	0.97
69.61	15.73	5.00	2.78	2.00	2.52	1.36	1.01
68.18	15.11	5.32	3.74	2.73	2.44	1.55	0.94
80.56	8.76	4.23	1.77	0.87	2.19	0.74	0.87
70.61	15.68	6.33	1.63	1.07	2.44	1.05	1.21
76.17	10.39	5.88	1.90	1.39	2.57	0.69	1.01
68.02	18.04	6.57	1.19	1.31	2.43	1.25	1.20
63.40	18.56	5.96	4.03	3.33	2.06	1.60	1.08
82.20	8.56	3.01	1.73	1.07	1.69	0.58	0.82
78.43	11.75	4.86	0.96	0.95	1.88	0.72	0.79

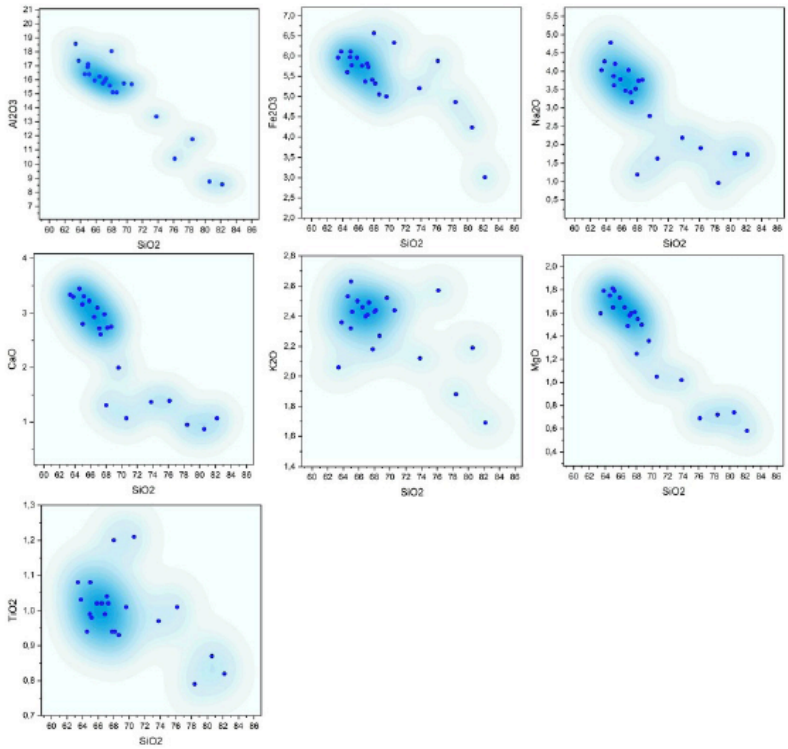

Figure 6: Clustering of oxides concentration downstream the Amazon River obtained from Martinelli *et al*. [11].

shifts in the relative proportions of minerals, oxides, and trace elements are expected, with potential consequences for water quality, ecosystem functioning, and human health [16, 36, 37].

Overall, the integrated mineralogical and chemical signatures observed in the Acre River sediments highlight both the long-term geomorphic evolution of the basin and the emerging influence of anthropogenic disturbances. These findings underscore the need for continued monitoring and expanded datasets to better understand ongoing environmental changes in southwestern Amazonia.

5. CONCLUSION

This study provides a detailed chemical and mineralogical characterization of suspended sediments in the Acre River, offering one of the first integrated datasets for a poorly studied southwestern Amazonian tributary. The results confirm the strong Andean geological influence on the Acre River sediment load, with mineral assemblages dominated by quartz and kaolinite, consistent with other Amazonian whitewater systems. The presence of all 16 natural REEs and their downstream enrichment patterns highlight long-term weathering processes and sediment transport dynamics that connect local catchments to the broader Amazon Basin.

The enrichment factor analysis indicates clear anthropogenic contributions to several trace elements (V, Tl, Co, Ni, Ga, Rb, Bi, Cd, Cr, Cs, Li, and As), revealing that human activities are already influencing sediment composition in the region. Although Hg was not detected, its absence is notable given known emissions in adjacent basins. The clustering of major oxides (SiO_2, Al_2O_3, Fe_2O_3, CaO, MgO, K_2O, Na_2O, TiO_2) demonstrates consistent geochemical behavior among whitewater rivers and provides a potential baseline for future temporal and spatial monitoring.

Together, these findings underscore the dual control of natural geological processes and emerging anthropogenic pressures on sediment geochemistry in the Acre River Basin. By integrating REE signatures, mineralogical profiles, and trace metal enrichment patterns, this work advances our understanding of sediment provenance, weathering intensity, and human impacts in a rapidly changing Amazon landscape. The dataset presented here establishes a foundation for long-term environmental assessments and contributes critical information for evaluating ongoing and future alterations in the basin's hydrogeochemical balance.

AUTHORS' CONTRIBUTION

Alejandro Duarte: Conceptualization, Investigation, Writing – Original Draft.
(https: //orcid.org/0000-0001-5527-703X)

Enrique Roy Dionisio Calderon: Formal Analysis, Data Curation.
(https: //orcid.org/0000-0002-0296-6242)

Roberto R. de Avillez: Formal Analysis, Data Curation. (https: //orcid.org/0000-0002-2192-1082)

Bruno Siciliano: Writing – Original Draft, Writing – Review & Editing.
(https: //orcid.org/0000-0002-9932-0607)

Adriana Gioda: Supervision, Writing – Review & Editing. (https: //orcid.org/0000-0002-5315-5650)

CONFLICT OF INTEREST STATEMENT

The Authors declare that there are no relevant financial or non-financial competing interests to report.

FUNDING STATEMENT

This study was financed in part by the Coordenação de Aperfeiçoamento de Pessoal de Nível Superior - Brasil (CAPES) - Finance Code 001. A. Gioda thanks FAPERJ for the Auxílio Cientista do Nosso Estado and CNPq for the Bolsa de Produtividade. B. Siciliano thanks to CNPq for Postdoc fellowship.

REFERENCES

[1] Guayasamin JM, Ribas CC, Carnaval AC, Carrillo JD, Hoorn C, Lohmann LG, *et al*. Evolution of Amazonian biodiversity: A review. Acta Amazon. 2024; 54. https://doi.org/10.1590/1809-4392202103601

[2] Park E, Latrubesse EM. Surface water types and sediment distribution patterns at the confluence of mega rivers: The Solimões Amazon and Negro Rivers junction. Water Resour Res. 2015; 51: p. 6197-213. https://doi.org/10.1002/2014WR016757

[3] Quesada CA, Lloyd J, Anderson LO, Fyllas NM, Schwarz M, Czimczik CI. Soils of Amazonia with particular reference to the RAINFOR sites. Biogeosciences. 2011; 8: p. 1415-40. https://doi.org/10.5194/bg-8-1415-2011

[4] Lucas Y, Montes CR, Mounier S, Loustau-Cazalet M, Ishida D, Achard R, *et al*. Biogeochemistry of an amazonian podzol-ferralsol soil system with white kaolin. 2012. https://doi.org/10.5194/bgd-9-2233-2012

[5] Bardy M, Derenne S, Allard T, Benedetti MF, Fritsch E. Podzolisation and exportation of organic matter in black waters of the Rio Negro (upper Amazon basin, Brazil). Biogeochemistry. 2011; 106: p. 71-88. https://doi.org/10.1007/s10533-010-9564-9

[6] Allard T, Ponthieu M, Weber T, Filizola N, Guyot JL, Benedetti M. Nature et propriétés de solides en suspension du Bassin amazonien. Bulletin de la Societe Geologique de France. 2002; 173: p. 67-75. https://doi.org/10.2113/173.1.67

[7] Leenheer JA, Santos U de M. Considerações sobre os processos de sedimentação na água preta ácida do rio Negro (Amazônia Central). Acta Amazon. 1980; 10: p. 343-57. https://doi.org/10.1590/1809-43921980102343

[8] Queiroz MMA, Horbe AMC, Seyler P, Moura CAV. Hidroquímica do rio Solimões na região entre Manacapuru e Alvarães: Amazonas - Brasil. Acta Amazon. 2009; 39: p. 943-52. https://doi.org/10.1590/S0044-59672009000400022

[9] Ríos-Villamizar EA, Adeney JM, Piedade MTF, Junk WJ. New insights on the classification of major Amazonian river water types. Sustain Water Resour Manag. 2020; 6: 83. https://doi.org/10.1007/s40899-020-00440-5

[10] Barton C, Karathanasis A. Clay Minerals. In: Dekker M, editor. Encyclopedia of Soil Science. 2002. p. 187-92.

[11] Martinelli LA, Victoria RL, Dematte JLI, Richey JE, Devol AH. Chemical and mineralogical composition of Amazon River floodplain sediments, Brazil. Applied Geochemistry. 1993; 8: p. 391-402. https://doi.org/10.1016/0883-2927(93)90007-4

[12] Barthelmy D. Mineralogy Database. 2014. Available from https: //webmineral.com/ [cited 2025 Oct 21]

[13] Gerard M, Seyler P, Benedetti MF, Alves VP, Boaventura GR, Sondag F. Rare earth elements in the Amazon basin. Hydrol Process. 2003; 17: 1379-92. https://doi.org/10.1002/hyp.1290

[14] Guyot JL, Jouanneau JM, Soares L, Boaventura GR, Maillet N, Lagane C. Clay mineral composition of river sediments in the Amazon Basin. Catena (Amst). 2007; 71: p. 340-56. https://doi.org/10.1016/j.catena.2007.02.002

[15] Wysocka I. Determination of rare earth elements concentrations in natural waters - A review of ICP-MS measurement approaches. Talanta. 2021; 221: p. 121636. https://doi.org/10.1016/j.talanta.2020.121636

[16] Pinto FG, Junior RE, Saint'Pierre TD. Sample Preparation for Determination of Rare Earth Elements in Geological Samples by ICP-MS: A Critical Review. Anal Lett. 2012; 45: p. 1537-56. https://doi.org/10.1080/00032719.2012.677778

[17] Duarte AF, Gioda A. Inorganic composition of suspended sediments in the Acre River, Amazon Basin, Brazil. Latin American Journal of Sedimentology and Basin Analysis. 2014; 21: p. 3-15.

[18] Doebelin N, Kleeberg R. Profex: a graphical user interface for the Rietveld refinement program *BGMN*. J Appl Crystallogr. 2015; 48: p. 1573-80. https://doi.org/10.1107/S1600576715014685

[19] Hu Z, Gao S. Upper crustal abundances of trace elements: A revision and update. Chem Geol. 2008; 253: p. 205-21. https://doi.org/10.1016/j.chemgeo.2008.05.010

[20] Chen J, Gaillardet J, Bouchez J, Louvat P, Wang Y. Anthropophile elements in river sediments: Overview from the Seine River, France. Geochemistry, Geophysics, Geosystems. 2014; 15: p. 4526-46. https://doi.org/10.1002/2014GC005516

[21] Ramos SJ, Dinali GS, Oliveira C, Martins GC, Moreira CG, Siqueira JO, *et al*. Rare Earth Elements in the Soil Environment. Curr Pollut Rep. 2016; 2: p. 28-50. https://doi.org/10.1007/s40726-016-0026-4

[22] Ramasamy V, Rajkumar P, Ponnusamy V. Depth wise analysis of recently excavated Vellar river sediments through FTIR and XRD studies. Indian Journal of Physics. 2009; 83: p. 1295-308. https://doi.org/10.1007/s12648-009-0110-3

[23] Murugesan S, Ramasamy V, Mullainathan S. Characterisation of minerals and relative distribution of quartz in Cauvery river sediments from Tamilnadu, India - A FTIR Study. Bulletin of Pure and Applied Sciences. 2004. https: //www.researchgate.net/publication/318310805

[24] Moreira-Turcq P, Seyler P, Guyot J-L. Characterization of suspended particulates and dissolved adsorbed organic matter in Amazon river. 2014. https: //www.researchgate.net/publication/235451859

[25] Bergmann J. Modern crystallographic algorithms and data structures (a very personal approach). 2021. Available from https: //www.iucr.org/resources/commissions/computing/newsletters/1/modern-crystallographic-algorithms [cited 2025 Oct 17]

[26] United States Geological Survey. Mineral commodity summaries 2025. 2025. Available from.

[27] Brioschi L, Steinmann M, Lucot E, Pierret MC, Stille P, Prunier J, *et al*. Transfer of rare earth elements (REE) from natural soil to plant systems: implications for the environmental availability of anthropogenic REE. Plant Soil. 2013; 366: p. 143-63. https://doi.org/10.1007/s11104-012-1407-0

[28] Silva FBV, Nascimento CWA, Alvarez AM, Araújo PRM. Inputs of rare earth elements in Brazilian agricultural soils via P-containing fertilizers and soil correctives. J Environ Manage. 2019; 232: p. 90-6. https://doi.org/10.1016/j.jenvman.2018.11.031

[29] Edahbi M, Plante B, Benzaazoua M, Ward M, Pelletier M. Mobility of rare earth elements in mine drainage: Influence of iron oxides, carbonates, and phosphates. Chemosphere. 2018; 199: p. 647-54. https://doi.org/10.1016/j.chemosphere.2018.02.054

[30] Kanazawa Y, Kamitani M. Rare earth minerals and resources in the world. J Alloys Compd. 2006; 408-412: p. 1339-43. https://doi.org/10.1016/j.jallcom.2005.04.033

[31] Emsbo P, McLaughlin PI, Breit GN, du Bray EA, Koenig AE. Rare earth elements in sedimentary phosphate deposits: Solution to the global REE crisis? Gondwana Research. 2015; 27: p. 776-85. https://doi.org/10.1016/j.gr.2014.10.008

[32] Forsyth K, Dia A, Marques R, Prudêncio MI, Obregón-Castro C, Diamantino C, *et al*. Relationship between the distribution of rare earth elements in soil pools with plant uptake: a sequential extraction study. Plant Soil. 2024. https://doi.org/10.1007/s11104-024-07135-2

[33] Balogh-Brunstad Z, Keller CK, Bormann BT, O'Brien R, Wang D, Hawley G. Chemical weathering and chemical denudation dynamics through ecosystem development and disturbance. Global Biogeochem Cycles. 2008; 22. https://doi.org/10.1029/2007GB002957

[34] Bouchez J, Moquet J, Espinoza JC, Martinez J, Guyot J, Lagane C, *et al*. River Mixing in the Amazon as a Driver of Concentration□Discharge Relationships. Water Resour Res. 2017; 53: p. 8660-85. https://doi.org/10.1002/2017WR020591

[35] Vital H, Stattegger K, Garbe-Schoenberg C-D. Composition and trace-element geochemistry of detrital clay and heavy-mineral suites of the lowermost Amazon River; a provenance study. Journal of Sedimentary Research. 1999; 69: p. 563-75. https://doi.org/10.2110/jsr.69.563

[36] Davidson EA, de Araújo AC, Artaxo P, Balch JK, Brown IF, C. Bustamante MM, *et al*. The Amazon basin in transition. Nature. 2012; 481: p. 321-8. https://doi.org/10.1038/nature10717

[37] Ellwanger JH, Kulmann-Leal B, Kaminski VL, Valverde-Villegas JM, Veiga ABG Da, Spilki FR, *et al*. Beyond diversity loss and climate change: Impacts of Amazon deforestation on infectious diseases and public health. An Acad Bras Cienc. 2020; 92. https://doi.org/10.1590/0001-3765202020191375

https://doi.org/10.12974/2311-8741.2025.13.06